Preparation of group 15 (phosphorus, antimony, and bismuth) complexes of meso-tetra-p-tolylporphyrin (TTP) and X-ray crystal structure of [Sb(TTP)(OCH(CH3)2)2]Cl

5 AUTHORS, INCLUDING:

Warwick J. Belcher
University of Newcastle
109 PUBLICATIONS **1,833** CITATIONS

Penelope J Brothers
University of Auckland
84 PUBLICATIONS **1,960** CITATIONS

David C Ware
University of Auckland
50 PUBLICATIONS **1,029** CITATIONS

polarization mechanism must be operative also in this case. For NIToPy no safe conclusions can be reached about the relative efficiency of the pyridine and N–O exchange pathways. However, the largest J value observed for this radical may indicate a sizeable ferromagnetic coupling is transmitted through the pyridine ring.

Contribution from the Department of Chemistry,
University of Auckland, Private Bag, Auckland, New Zealand

Preparation of Group 15 (Phosphorus, Antimony, and Bismuth) Complexes of *meso*-Tetra-*p*-tolylporphyrin (TTP) and X-ray Crystal Structure of [Sb(TTP)(OCH(CH₃)₂)₂]Cl

Tanya Barbour, Warwick J. Belcher, Penelope J. Brothers,* Clifton E. F. Rickard, and David C. Ware

The syntheses of cationic phosphorus(V) and antimony(V) *meso*-tetra-*p*-tolylporphyrin (TTP) complexes [P(TTP)X₂]X (X = Cl, OH) and [Sb(TTP)X₂]X′ (X, X′: Cl, SbCl₆; Cl, Cl; OH, OH) and the bismuth(III) complex [Bi(TTP)]NO₃ are described. Reactions of the phosphorus and antimony chloro complexes with alcohols and primary amines produce the new alkoxo and aryloxo complexes [P(TTP)(OR)₂]X (R, X: CH₃, Cl; CH₂CH₃, Cl; CH(CH₃)₂, Cl; CH₂CH(CH₃)₂, Cl; CH₂C(CH₃)₃, Cl; *p*-C₆H₄CH₃, Cl; *p*-C₆H₄OH, OH; *o*-C₆H₄OH, OH) and [Sb(TTP)(OR)₂]Cl (R = CH₃, CH₂CH₃, CH(CH₃)₂, CH₂CH(CH₃)₂), and the amido complex [P(TTP)(NH-*p*-C₆H₄CH₃)₂]Cl. ³¹P NMR data recorded for the phosphorus porphyrin complexes reveal the marked upfield shift of the coordinated phosphorus atom, and unusual seven-bond P–H coupling in the complexes with *p*-tolyl substituents on the axial ligands. A variable-temperature ¹H NMR study of [Bi(TTP)]NO₃ permits observation on the NMR time scale of aryl ring rotation on the porphyrin periphery. The structure of [Sb(TTP)(OCH(CH₃)₂)₂]Cl was determined by a single-crystal X-ray structure analysis. It crystallizes in the space group $P\bar{1}$ with a = 13.515 (5) Å, b = 14.628 (4) Å, c = 15.709 (3) Å, α = 109.59 (2)°, β = 94.38 (2)°, γ = 102.19 (3)°, V = 2823 (1) Å³, and Z = 2. The structure was refined to R = 0.081 and R_w = 0.083. The Sb atom is displaced 0.030 Å from the mean porphyrin plane and the average Sb–O bond distance is 1.935 Å.

Introduction

Although the coordination of most of the metallic elements to the porphyrin macrocycle has been demonstrated, for many years it was transition-metal porphyrin complexes which were the focus of the most intense attention. More recently, there has been a resurgence of interest in main-group chemistry, driven by the search for new conducting materials and new chemotherapeutic agents and the recent discovery of previously unsuspected bonding modes for main-group elements. Porphyrin complexes of the main-group elements have not been excluded from this renewed interest, and there has been recent activity in the study of elements from groups 13 and 14 coordinated to the porphyrin macrocycle.[1]

The insertion of antimony into mesoporphyrin dimethyl ester and etioporphyrin in 1969 provided the first examples of porphyrin complexes containing a group 15 element.[2] However, both this report and a 1974 paper describing the preparation of arsenic, antimony, and bismuth octaethylporphyrin complexes[3] engendered some confusion regarding the formulation of the products and the oxidation state of the central element. A later review correctly assigns the oxidation state and cationic nature of the six-coordinate arsenic(V) and antimony(V) complexes [E(Por)X₂]⁺ (E = As, Sb; X = halide, OH⁻) and the bismuth(III) complex [Bi-(OEP)]NO₃.[4,5] Although both this review[4] and another account[6]

refer to the preparation of a number of arsenic, antimony, and bismuth tetraarylporphyrin complexes, there have been no experimental details reported in the primary literature for any porphyrin species containing these elements since the 1969 and 1974 accounts in which the products were incorrectly characterized.[2,3] However, the formulation of the antimony species has been confirmed by an X-ray crystal structure analysis of [Sb-(OEP)(OH)₂]ClO₄·CH₃CH₂OH.[7]

In contrast to the rather poorly documented heavier group 15 element porphyrin complexes, the coordination of the lighter element phosphorus to the porphyrin macrocycle has received some attention. The insertions of phosphorus into H₂TPP[8] and H₂OEP[9] were reported by independent workers in 1977. Since then, the spectroscopic and electrochemical behavior of the [P(Por)X₂]⁺ (X = OH⁻, Cl⁻) ion has been reported[10–14] along with an X-ray crystal structure determination of [P(TPP)(OH)₂]OH·2H₂O.[11]

The availability of two oxidation states for the elements P, As, and Sb offers the possibility of redox chemistry of the coordinated element. In fact, UV/visible spectroscopic data have been observed for reactive but poorly characterized species proposed to be phosphorus(III), arsenic(III), and antimony(III) porphyrin com-

(1) (a) Guilard, R.; Kadish, K. M. *Chem. Rev.* **1988**, *88*, 1121. (b) Guilard, R.; Lecomte, C.; Kadish, K. M. *Struct. Bonding* **1987**, *64*, 205. (c) Kadish, K. M. *Prog. Inorg. Chem.* **1986**, *34*, 435.
(2) Treibs, A. *Liebigs Ann. Chem.* **1969**, *728*, 115.
(3) Buchler, J. W.; Lay, K. L. *Inorg. Nucl. Chem. Lett.* **1974**, *10*, 297.
(4) Sayer, P.; Gouterman, M.; Connell, C. R. *Acc. Chem. Res.* **1982**, *15*, 73.
(5) Abbreviations for porphyrinato dianions: Por, unspecified; Etio, etio-porphyrinato; MPDME, dianion of mesoporphyrin dimethyl ester; OEP, octaethylporphyrinato; TPP, *meso*-tetraphenylporphyrinato; TTP, *meso*-tetra-*p*-tolylporphyrinato.

(6) Buchler, J. W. In *The Porphyrins*; Dolphin, D., Ed.; Academic Press: New York, 1978; Vol. 1, Chapter 10.
(7) Fitzgerald, A; Stenkamp, R. E.; Watenpugh, K. D.; Jensen, L. H. *Acta Crystallogr.* **1977**, *B33*, 1688.
(8) Carrano, C. J.; Tsutsui, M. *J. Coord. Chem.* **1977**, *7*, 79.
(9) Sayer, P.; Gouterman, M.; Connell, C. R. *J. Am. Chem. Soc.* **1977**, *99*, 1082.
(10) Marrese, C. A.; Carrano, C. J. *J. Chem. Soc., Chem. Commun.* **1982**, 1279.
(11) Mangani, S.; Meyer, E. F.; Cullen, D. L.; Tsutsui, M.; Carrano, C. J. *Inorg. Chem.* **1983**, *22*, 400.
(12) Marrese, C. A.; Carrano, C. J. *Inorg. Chem.* **1983**, *22*, 1858.
(13) Marrese, C. A.; Carrano, C. J. *Inorg. Chem.* **1984**, *23*, 3961.
(14) Gouterman, M.; Sayer, P.; Shankland, E.; Smith, J. P. *Inorg. Chem.* **1981**, *20*, 87.

Table I. Crystallographic Data for [Sb(TTP)(OCH(CH₃)₂)₂]Cl **(13)**

formula	$C_{54}H_{50}ClN_4O_2Sb$	V, Å³	2823.0 (1.0)
M_r	943.20	ρ_{calcd}, g·cm⁻³	1.11
space group	$P\bar{1}$	Z	2
a, Å	13.515 (5)	T, °C	20
b, Å	14.628 (4)	λ, Å	0.71069
c, Å	15.709 (3)	μ, cm⁻¹	5.8
α, deg	109.59 (2)	transm coeff	0.94–1.00
β, deg	94.38 (2)	R^a	0.081
γ, deg	102.19 (3)	$R_w{}^b$	0.083

$^a R = \sum||F_o| - |F_c||/\sum|F_o|$. $^b R_w = [\sum_w(|F_o| - |F_c|)^2/\sum_w|F_o|^2]^{1/2}$, $w = 1.0/[\sigma^2(F_o) + 0.020F_o^2]$.

plexes.[4] In particular, the absorption spectrum of the latter species is very similar to that of the enzyme cytochrome P-450, and this comparison has received some attention.[15] The non-metal status of phosphorus and the observation that the phosphorus(V) ion is the smallest ever to have been inserted into the porphyrin ring have contributed to the interest in complexes of this element. The bismuth(III) ion is by contrast much larger than the porphyrin ligand cavity, giving within group 15 a range from a very small, light non-metal ion to a large, heavy metal ion coordinated to a porphyrin ligand.

Although the above studies have focussed on features of the phosphorus(V), arsenic(V), and antimony(V) porphyrin halide and hydroxide derivatives, little attention has been paid to the reaction chemistry of these complexes. We have explored the chemical reactivity of these and the bismuth porphyrin complexes. As part of this study we report full experimental details for the preparation of phosphorus(V), antimony(V), and bismuth(III) tetra-*p*-tolylporphyrin complexes. This represents the first full report of tetraarylporphyrin complexes of the latter two elements. We were unsuccessful in inserting arsenic into H₂TTP. A series of alkoxo and aryloxo derivatives of phosphorus and antimony and, in the case of phosphorus, an arylamido derivative are described, further elaborating the range of ligands coordinated in the axial sites of these complexes. An X-ray crystal structure determination of [Sb(TTP)(OCH(CH₃)₂)₂]Cl and a variable-temperature ¹H NMR study of [Bi(TTP)]NO₃ are also discussed.

Experimental Section

Materials and Measurements. All solvents were dried and distilled prior to use. Pyridine was distilled under nitrogen from calcium hydride. H₂TTP was prepared by literature methods.[16] All reactions were carried out under a nitrogen atmosphere, and subsequent isolation and purification procedures were carried out in air. Samples for elemental analysis were dried under vacuum over P₂O₅ at room temperature. Melting points were determined on a Reichert Kofler microscope hot stage and are uncorrected. UV–visible absorption spectra were recorded on a Varian DMS 100 spectrophotometer. ¹H and ³¹P NMR spectra were recorded on a Bruker AM 400 spectrometer operating at 400 and 162 MHz, respectively. FAB mass spectra were recorded from a glycerol matrix on a VG 70-SE mass spectrometer using argon gas. IR spectra (4000–200 cm⁻¹) were recorded as nujol mulls between KBr or CsI plates on a Perking-Elmer 597 double-beam spectrophotometer calibrated with polystyrene film. Elemental analyses were performed by Dr. R. G. Cunninghame and associates at the University of Otago and are gratefully acknowledged.

All diffraction data for the structure determination of [Sb(TTP)(O-CH(CH₃)₂)₂]Cl **(13)** were collected on an Enraf-Nonius CAD-4 diffractometer using graphite-monochromated Mo Kα (λ = 0.71069 Å) radiation. The structure was solved using the SHELX-76 program and refined to final residuals R = 0.081 and R_w = 0.083. Crystallographic data are given in Table I and positional parameters are given in Table II. Further crystallographic data and details of the structure solution are given in the supplementary material, together with atomic thermal parameters and the observed and calculated structure factors.

Syntheses. [P(TTP)Cl₂]Cl (1). POCl₃ (8 mL) was added dropwise to a solution of H₂TTP (3.00 g) in pyridine (50 mL) and the resulting solution was heated at reflux temperature for 24 h. The pyridine and excess POCl₃ were removed under low pressure leaving a purple solid.

Table II. Positional Parameters with Estimated Standard Deviations for [Sb(TTP)(OCH(CH₃)₂)₂]Cl **(13)**

atom	x/a	y/b	z/c	G
Sb	0.4198 (5)	0.24055 (5)	0.31214 (4)	
N1	0.6096 (7)	0.2948 (6)	0.2722 (6)	
N2	0.3917 (6)	0.2383 (6)	0.1931 (6)	
N3	0.5533 (7)	0.2435 (6)	0.4302 (6)	
N4	0.3352 (6)	0.1834 (6)	0.3494 (6)	
O1	0.4906 (5)	0.1076 (5)	0.2553 (5)	
O2	0.4666 (6)	0.3761 (5)	0.3828 (5)	
C1	0.7304 (8)	0.3025 (8)	0.4069 (7)	
C2	0.6593 (8)	0.2677 (7)	0.4534 (7)	
C3	0.6819 (8)	0.2504 (8)	0.5380 (7)	
C4	0.5911 (8)	0.2153 (8)	0.5628 (8)	
C5	0.5080 (7)	0.2097 (7)	0.4953 (7)	
C6	0.4074 (8)	0.1700 (7)	0.4935 (7)	
C7	0.3282 (9)	0.1593 (8)	0.4269 (8)	
C8	0.2181 (9)	0.1182 (9)	0.4252 (8)	
C9	0.1633 (8)	0.1182 (8)	0.3478 (8)	
C10	0.2386 (8)	0.1596 (7)	0.2996 (7)	
C11	0.2135 (8)	0.1758 (7)	0.2182 (7)	
C12	0.2848 (8)	0.2103 (8)	0.1690 (7)	
C13	0.2598 (9)	0.2259 (9)	0.0855 (8)	
C14	0.3496 (9)	0.2649 (8)	0.0623 (7)	
C15	0.4331 (9)	0.2721 (7)	0.1273 (6)	
C16	0.5372 (9)	0.3084 (8)	0.1278 (7)	
C17	0.6201 (8)	0.3175 (8)	0.1945 (7)	
C18	0.7234 (8)	0.3551 (9)	0.1946 (8)	
C19	0.7733 (9)	0.3510 (9)	0.2678 (8)	
C20	0.7061 (8)	0.3153 (8)	0.3201 (7)	
C21	0.8415 (8)	0.3259 (8)	0.4419 (7)	
C22	0.9047 (9)	0.2762 (9)	0.3887 (9)	
C23	1.0080 (11)	0.2991 (11)	0.4252 (10)	
C24	1.0494 (10)	0.3675 (10)	0.5156 (11)	
C25	0.9848 (9)	0.4132 (10)	0.5634 (9)	
C26	0.8832 (9)	0.3950 (9)	0.5281 (8)	
C27	0.3755 (8)	0.1373 (9)	0.5718 (8)	
C28	0.3472 (13)	0.1999 (11)	0.6448 (10)	
C29	0.3148 (13)	0.1712 (13)	0.7157 (10)	
C30	0.3149 (11)	0.0694 (12)	0.7126 (10)	
C31	0.3487 (13)	0.0130 (12)	0.6406 (12)	
C32	0.3784 (12)	0.0452 (10)	0.5716 (10)	
C33	0.1045 (9)	0.1504 (9)	0.1782 (8)	
C34	0.0462 (10)	0.0541 (10)	0.1407 (9)	
C35	−0.0594 (11)	0.0373 (12)	0.1031 (9)	
C36	−0.1002 (10)	0.1098 (13)	0.0960 (10)	
C37	−0.0409 (11)	0.2068 (12)	0.1329 (9)	
C38	0.0571 (10)	0.2275 (10)	0.1739 (9)	
C39	0.5646 (9)	0.3467 (9)	0.0533 (8)	
C40	0.5386 (12)	0.2830 (10)	−0.0391 (10)	
C41	0.5642 (13)	0.3196 (10)	−0.1070 (9)	
C42	0.6140 (13)	0.4199 (12)	−0.0865 (10)	
C43	0.6370 (12)	0.4840 (11)	0.0042 (10)	
C44	0.6143 (11)	0.4479 (9)	0.0733 (9)	
C45	0.4448 (9)	0.4486 (8)	0.3481 (7)	
C46	0.5384 (11)	0.5382 (9)	0.3749 (11)	
C47	0.3509 (12)	0.4778 (11)	0.3810 (10)	
C48	0.4150 (9)	0.0237 (9)	0.1904 (9)	
C49	0.4513 (13)	−0.0049 (14)	0.1006 (11)	
C50	0.3954 (16)	−0.0564 (12)	0.2255 (15)	
C51	1.1610 (11)	0.3880 (12)	0.5512 (11)	
C52	0.2818 (14)	0.0388 (14)	0.7847 (12)	
C53	−0.2080 (13)	0.0791 (13)	0.0464 (12)	
C54	0.6425 (18)	0.4554 (16)	−0.1616 (15)	
Cl	0.9458 (19)	0.024 (2)	0.4483 (19)	0.25 (1)
Cl	0.1340 (11)	0.2553 (10)	0.8952 (10)	0.43 (1)
Cl	0.031 (2)	0.049 (2)	0.589 (2)	0.20 (1)
Cl	−0.034 (3)	0.086 (3)	0.525 (3)	0.16 (1)

This was dissolved in a minimum of dichloromethane and chromatographed on silica gel (100 g). Elution with dichloromethane removed a pale red band containing unreacted H₂TTP. The desired product was then eluted as a purple band using CH₃OH–CH₂Cl₂ (1:9). In some cases the compound was chromatographed twice to obtain a pure product. The solvent was removed to give the product as a glassy amorphous solid film. The addition of benzene to this film and stirring resulted in crystallization of **1** as fine purple crystals (3.23 g, 83%). Anal. Calcd for $C_{48}H_{36}Cl_3N_4P \cdot C_6H_6 \cdot H_2O$: C, 71.88; H, 4.91; N, 6.21. Found: C, 71.67;

(15) Hanson, L. K.; Eaton, W. A.; Sligar, S. G.; Gunsalus, I. C.; Gouterman, M.; Connell, C. R. *J. Am. Chem. Soc.* **1976**, *98*, 2672.

(16) Fuhrhop, J.-H.; Smith, K. M. In *Porphyrins and Metalloporphyrins*; Smith, K. M., Ed.; Elsevier: Amsterdam, 1975; p 769.

H, 5.34; N, 6.14. UV–visible (CH$_2$Cl$_2$): λ_{max} (log ϵ), 443.5 (5.46), 571.2 (4.14), 617.1 (4.01) nm. IR (Nujol): 425 cm^{-1} (ν_{P-Cl}). MS (m/z): [M]$^+$, 769; [M – H, Cl]$^+$, 733; [M – 2Cl]$^+$, 699 (base peak).

[Sb(TTP)Cl$_2$]SbCl$_6$ (2a) and [Sb(TTP)Cl$_2$]Cl (2b). SbCl$_5$ (0.85 mL) was added to a solution of H$_2$TTP (0.67 g) in pyridine (50 mL), and the resulting solution was refluxed for 30 min, at which time disappearance of the H$_2$TTP bands in the UV–visible spectrum indicated that the reaction was complete. The pyridine and excess SbCl$_5$ were removed under low pressure, and the resulting purple solid was dissolved in a minimum of dichloromethane and chromatographed on Florisil (100 g). Elution with dichloromethane removed any H$_2$TTP present. The desired compound was then eluted as a purple band using methanol–dichloromethane (1:19). (Chromatography on silica gel resulted in considerable conversion to a second compound subsequently identified as [Sb(TTP)Cl$_2$]Cl (2b).) Removal of the solvent and recrystallization from dichloromethane/ ethanol resulted in irregular purple crystals of the hexachloroanimonate salt 2a. (0.992 g, 83%). Mp: 266–269 °C dec. Anal. Calcd for C$_{48}$H$_{36}$Cl$_8$N$_4$Sb$_2$: C, 48.21; H, 3.03; N, 4.69; Cl, 23.72. Found: C, 48.16; H, 3.64; N, 4.48; Cl, 24.01. UV–visible (CH$_2$Cl$_2$): λ_{max} (log ϵ), 431.2 (5.55), 319.5 (4.42), 558.0 (4.27), 601.5 (4.29) nm. IR (Nujol): 350 cm^{-1} (ν_{Sb-Cl}, cation); 325, 330, 335 cm^{-1} (ν_{Sb-Cl}, SbCl$_6^-$). MS (m/z): [M]$^+$, 861 (^{123}Sb); [M]$^+$, 859 (^{121}Sb); [M – 2Cl]$^+$, 791 (^{123}Sb).

[Sb(TTP)Cl$_2$]SbCl$_6$ (2a) (0.100 g) was dissolved in a minimum amount of methanol–dichloromethane (1:1) and loaded on to Amberlite Resin IRA-401 ion-exchange resin (chloride form, 1 g) which had been soaked in water and rinsed wth methanol–dichloromethane (1:1). Elution with methanol–dichloromethane (1:1) and subsequent removal of the solvent resulted in a purple solid. This was recrystallized from hexane–dichloromethane to give diamond-shaped purple crystals of the chloride salt 2b (0.077 g, 97%). Mp: >300 °C. Anal. Calcd for C$_{48}$H$_{36}$Cl$_3$N$_4$Sb·3H$_2$O: C, 60.62; H, 4.45; N, 5.89; Cl, 11.18. Found: C, 60.57; H, 4.77; N, 5.77; Cl, 11.01. UV–visible (CH$_2$Cl$_2$): λ_{max} (log ϵ), 431.2 (5.55), 319.5 (4.42), 558.0 (4.27), 601.5 (4.29) nm. IR (Nujol): 350 cm^{-1} (ν_{Sb-Cl}).

[Bi(TTP)]NO$_3$ (3). A solution of bismuth nitrate (5.20 g) and H$_2$TTP (0.67 g) in pyridine (50 mL) was heated under reflux for 30 min. During this period the solution changed color from dark purple to olive green. The pyridine was removed under reduced pressure, giving a dark green solid. This was dissolved in a minimum of dichloromethane and chromatographed on silica gel (100 g). Elution with dichloromethane removed a faint red fraction containing H$_2$TTP. The desired product was then eluted from the column as a dark green band using methanol–dichloromethane (1:19). The addition of ethanol followed by reduction of the solvent volume gave green crystals of the nitrate salt 3 (0.712 g, 72%). Mp: 279–281 °C. Anal. Calcd for C$_{48}$H$_{36}$BiN$_5$O$_3$·C$_2$H$_4$OH: C, 60.91; H, 4.29; N, 7.10. Found: C, 60.83; H, 4.51; N, 6.94. UV–visible (CH$_2$Cl$_2$): λ_{max} (log ϵ), 469.4 (5.18), 353.7 (4.59), 601.4 (3.93), 650.1 (4.09) nm. MS (m/z): [M]$^+$, 877 (base peak).

[P(TTP)(OH)$_2$]OH (4). [P(TTP)Cl$_2$]Cl (1) (0.200 g) was dissolved in pyridine (50 mL) and water (5 mL) and refluxed for 12 h. Over this period the solution changed color from dark purple to dark crimson. The pyridine and water were removed under reduced pressure, and the red residue was chromatographed on silica gel (50 g). Elution with methanol–dichloromethane (1:9) removed the desired product as a red band, and no other bands were observed. The solvent was removed under reduced pressure to give a thin red glass. The addition of benzene and stirring resulted in crystallization as small red crystals (0.177 g, 89%). Anal. Calcd for C$_{48}$H$_{39}$N$_4$O$_3$P·C$_6$H$_6$·2H$_2$O: C, 74.98; H, 5.71; N, 6.48. Found: C, 74.64; H, 5.38; N, 6.25. UV–visible (pyridine): λ_{max} (log ϵ), 431.2 (5.45), 577.2 (4.21), 600.0 (3.93) nm. IR (Nujol): 905 cm^{-1} (ν_{P-O}). MS (m/z): [M – H]$^+$, 732 (base peak); [M – OH, H]$^+$, 715; [M – 2OH]$^+$, 699.

[Sb(TTP)(OH)$_2$](OH) (5). [Sb(TTP)Cl$_2$]SbCl$_6$ (2a) (0.200 g) was dissolved in pyridine (50 mL) and water (5 mL) and refluxed for 12 h. Over this period the solution changed color from dark purple to dark crimson. The solvents were removed under reduced pressure, and the red residue was chromatographed on silica gel (50 g). Elution with methanol–dichloromethane (1:9) resulted in three bands. The first, major band contained the desired product. The two minor bands contained [Sb-(TTP)Cl$_2$]SbCl$_6$ (2a) and [Sb(TTP)Cl$_2$]Cl (2b). The solvent was removed from the desired fraction and upon addition of benzene a flocculent red powder resulted. This was collected by filtration and washed with hexane (0.156 g, 83%). Anal. Calcd for C$_{48}$H$_{39}$N$_4$O$_3$Sb·2H$_2$O: C, 65.69; H, 4.94; N, 6.38. Found: C, 65.28; H, 5.17; N, 6.78. UV–visible (CH$_2$Cl$_2$): λ_{max} (log ϵ), 423.6 (5.55), 327.8 (4.00), 553.3 (4.14), 595.2 (4.03) nm. IR (Nujol): 1070 cm^{-1} (ν_{Sb-O}). MS (m/z): [M]$^+$, 823 (^{121}Sb); [M – OH, H]$^+$, 805 (^{121}Sb); [M – 2OH]$^+$, 789 (^{121}Sb, base peak).

[P(TTP)(OCH$_3$)$_2$]Cl (6). [P(TTP)Cl$_2$]Cl (1) (0.100 g) was dissolved in a mixture of pyridine (10 mL) and methanol (10 mL) and refluxed

for 12 h. The solvent was removed under reduced pressure and the red residue was chromatographed on silica gel (30 g). Elution with methanol:dichloromethane (1:9) removed the desired product. The solvent was removed under reduced pressure and the compound was recrystallized from benzene/octane to give fine needlelike red crystals (0.094 g, 98%). Anal. Calcd for C$_{50}$H$_{42}$ClN$_4$P·2H$_2$O: C, 72.06; H, 5.56; N, 6.72. Found: C, 72.43; H, 6.23; N, 6.35. UV–visible (CH$_2$Cl$_2$): λ_{max} (log ϵ), 443.5 (5.45), 571.2 (4.22), 616.1 (4.11) nm. IR (Nujol): 1040 cm^{-1} (ν_{P-O}). MS (m/z): [M]$^+$, 761 (base peak); [M – CH$_3$]$^+$, 746; [M – OCH$_3$]$^+$, 730; [M – OCH$_3$,CH$_3$]$^+$, 715; [M – 2OCH$_3$]$^+$, 699.

[P(TTP)(OCH$_2$CH$_3$)$_2$]Cl (7). [P(TTP)Cl$_2$]Cl (1) (0.100 g) was dissolved in a mixture of pyridine (10 mL) and ethanol (10 mL) and heated under reflux for 12 h. The product was isolated and purified as described for 6. Recrystallization from benzene/octane gave small red crystals (0.080 g, 81%). Anal. Calcd for C$_{52}$H$_{46}$ClN$_4$P·2H$_2$O: C, 72.34; H, 6.07; N, 6.49. Found: C, 71.82; H, 5.98; N, 6.25. UV–visible (CH$_2$Cl$_2$): λ_{max} (log ϵ), 441.5 (5.45), 569.2 (4.27), 614.1 (4.08) nm. IR (Nujol): 1065 cm^{-1} (ν_{P-O}). MS (m/z): [M – C$_2$H$_4$]$^+$, 761 (base peak); [M – 2C$_2$H$_5$]$^+$, 731; [M – OC$_2$H$_5$, C$_2$H$_5$]$^+$, 715; [M – 2OC$_2$H$_5$]$^+$, 699.

[P(TTP)(OCH(CH$_3$)$_2$)$_2$]Cl (8). [P(TTP)Cl$_2$]Cl (1) (0.03 g) was dissolved in a mixture of dry pyridine (5 mL) and dry 2-propanol (5 mL) and heated at reflux temperature for 4 h. The product was isolated and purified as described for 6. Recrystallization from benzene/octane yielded fine needlelike crystals (0.029 g, 91%). Anal. Calcd for C$_{54}$H$_{50}$ClN$_4$O$_2$P·3H$_2$O: C, 71.47; H, 6.22; N, 6.17. Found: C, 71.71; H, 5.87; N, 6.10. UV–visible (CH$_2$Cl$_2$): λ_{max} (log ϵ), 308.8 (3.9), 429.6 (5.3), 555.1 (3.9), 597.0 (3.6) nm. MS (m/z): [M + H]$^+$ 818; [818 – 2C$_3$H$_6$]$^+$, 734; [818 – OC$_3$H$_7$, C$_3$H$_7$]$^+$, 716.

[P(TTP)(OCH$_2$CH(CH$_3$)$_2$)$_2$]Cl (9). [P(TTP)Cl$_2$]Cl (1) (0.100 g) was dissolved in dry pyridine (15 mL) and dry isobutyl alcohol (3 mL) and heated at reflux temperature for 4 h. The solvent was removed, and the purple residue was recrystallized from CH$_2$Cl$_2$–toluene–octane yielding fine purple crystals (0.10 g, 91%). Anal. Calcd for C$_{56}$H$_{54}$ClN$_4$O$_2$P·CH$_2$Cl$_2$·3H$_2$O: C, 68.16; H, 6.22; N, 5.58. Found: C, 67.52; H, 6.47; N, 5.55. UV–visible (CH$_2$Cl$_2$): λ_{max} (log ϵ), 434.5 (5.6), 563.0 (4.4), 605.9 (4.6) nm. MS (m/z): [M + H]$^+$, 846 (base peak); [846 – OC$_4$H$_9$, C$_4$H$_9$], 716.

[P(TTP)(OCH$_2$C(CH$_3$)$_3$)$_2$]Cl (10). [P(TTP)Cl$_2$]Cl (1) (0.100 g) and neopentyl alcohol (0.4 g) were dissolved in dry pyridine (15 mL) and heated at reflux temperature for 4 h. The solvent was removed, and the purple residue was dissolved in dichloromethane and chromatographed on Florisil (30 g). H$_2$TTP was eluted using dichloromethane. Elution with methanol–dichloromethane (1:9) removed the desired product as a purple band. The solvent was removed, and the purple residue was recrystallized from CH$_2$Cl$_2$–toluene–octane (0.05 g, 55%). Anal. Calcd for C$_{58}$H$_{58}$ClN$_4$O$_2$P·2.5CH$_2$Cl$_2$: C, 64.77; H, 5.66. Found: C, 63.97; H, 5.20. UV–visible (CH$_2$Cl$_2$): λ_{max} (log ϵ), 434.5 (5.3), 561.3 (4.1), 609.2 (4.0) nm. MS (m/z): [M + H]$^+$, 874 (base peak); [874 – OC$_5$H$_{11}$, C$_5$H$_{11}$]$^+$, 716.

[Sb(TTP)(OCH$_3$)$_2$]Cl (11). [Sb(TTP)Cl$_2$]SbCl$_6$ (2a) (0.200 g) was dissolved in a mixture of pyridine (10 mL) and methanol (10 mL), and the solution was heated under reflux for 12 h. After removal of the solvent under reduced pressure, the purple-red residue was dissolved in benzene, filtered, and recrystallized from benzene/octane to give small purple-red crystals (0.153 g, 91%). Anal. Calcd for C$_{50}$H$_{42}$ClN$_4$O$_2$Sb·C$_6$H$_6$·2H$_2$O: C, 67.11; H, 5.23; N, 5.59. Found: C, 67.62; H, 5.46; N, 5.60. UV–visible (CH$_2$Cl$_2$): λ_{max} (log ϵ), 423.6 (5.54), 313.8 (4.44), 553.3 (4.38), 595.2 (4.33) nm. IR (Nujol): 585 cm^{-1} (ν_{Sb-O}). MS (m/z): [M]$^+$, 851 (^{121}Sb); [M – OCH$_3$, CH$_3$]$^+$, 805 (^{121}Sb); [M – 2OCH$_3$]$^+$, 789 (^{121}Sb, base peak).

[Sb(TTP)(OCH(CH$_3$)$_2$)$_2$]Cl (13). [Sb(TTP)Cl$_2$]Cl (2a) (0.100 g) was dissolved in dry pyridine (10 mL) and dry 2-propanol (10 mL) and heated at reflux temperature for 6 h. The product was isolated and purified as described for 6. Recrystallization from benzene–octane gave long needlelike crystals. (0.06 g, 57%). Anal. Calcd for C$_{54}$H$_{50}$ClN$_4$O$_2$Sb·3H$_2$O: C, 64.97; H, 5.66; N, 5.61. Found: C, 65.07; H, 5.54; N, 5.49. UV–visible (CH$_2$Cl$_2$): λ_{max} (log ϵ), 426.6 (5.6), 554.3 (4.3), 596.2 (4.3) nm. MS (m/z): [M]$^+$, 909 (^{123}Sb); [M – 2C$_3$H$_6$]$^+$, 825 (^{123}Sb); [M – 2OC$_3$H$_7$]$^+$, 791 (^{123}Sb).

[P(TTP)(O-p-C$_6$H$_4$CH$_3$)$_2$]Cl (15). [P(TTP)Cl$_2$]Cl (1) (0.100 g) and p-cresol (5 g) were dissolved in pyridine (20 mL) and refluxed for 30 min. The solvent was removed, and the purple residue was washed with hexane to remove most of the unreacted p-cresol. The resulting purple oil was chromatographed twice on silica gel (100 g). Elution with dichloromethane removed a faint red fraction containing H$_2$TTP. Elution with methanol–dichloromethane (1:9) removed the desired product as a purple band. The solvent was removed under reduced pressure, and the resulting purple solid was recrystallized from benzene–octane to give a purple-brown powder (0.076 g, 67%). Anal. Calcd for C$_{62}$H$_{50}$ClN$_4$O$_2$P·2.5H$_2$O: C, 74.88; H, 5.57; N, 5.63. Found: C, 74.89; H, 5.92; N, 5.63. IR

(Nujol): 885 cm^{-1} (ν_{P-O}). UV–visible (CH$_2$Cl$_2$): λ_{max} (log ϵ), 310.8 (4.16), 436.5 (5.11), 562.3 (4.06), 607.0 (3.78) nm. IR (Nujol): 885 cm^{-1} (ν_{P-O}). MS (m/z): [M + 2H]$^+$, 915; [915 – OC$_7$H$_8$]$^+$, 807; [M – 2OC$_7$H$_7$]$^+$, 699 (base peak).

P(TTP)(O-p-C$_6$H$_4$OH)$_2$]OH (16). [P(TTP)Cl$_2$]Cl (1) (0.100 g) and 1,4-dihydroxybenzene (1.0 g) were dissolved in pyridine (30 mL) and refluxed for 30 min. The solvent was removed and the residue was washed several times with a dilute aqueous solution of KOH. The crude product was then chromatographed twice on silica gel (100 g) as described for 15. The solvent was removed under reduced pressure to give a purple glassy film of amorphous solid. The addition of benzene to this glass with stirring resulted in crystallization as small purple crystals (0.088 g, 74%). Anal. Calcd for C$_{60}$H$_{47}$N$_4$O$_5$P·0.5C$_6$H$_6$·2H$_2$O: C, 74.91; H, 5.39; N, 5.55. Found: C, 74.86; H, 5.37; N, 5.54. UV–visible (CH$_2$Cl$_2$): λ_{max} (log ϵ), 428.6 (4.10), 563.5 (4.02), 608.2 (3.74) nm. IR (Nujol): 885 cm^{-1} (ν_{P-O}). MS (m/z): [M + H]$^+$, 918; [918 – OC$_6$H$_4$OH]$^+$, 809; [M – 2OC$_6$H$_4$OH]$^+$, 699 (base peak).

[P(TTP)(O-o-C$_6$H$_4$OH)$_2$]OH (17). [P(TTP)Cl$_2$]Cl (1) (0.100 g) and 1,2-dihydroxybenzene (1.0 g) were dissolved in pyridine (30 mL) and refluxed for 30 min. The solvent was removed, and the bulk of the unreacted catechol sublimed off by heating the residue under vacuum. The residue was then washed several times with an aqueous solution of KOH and then chromatographed as described for compound 16. The product was recrystallized from dichloromethane–benzene–octane to give a purple powder (0.082 g, 70%). Anal. Calcd for C$_{60}$H$_{47}$N$_4$O$_5$P·0.5C$_6$H$_6$·2H$_2$O: C, 74.91; H, 5.39; N, 5.55. Found: C, 74.79; H, 5.42; N, 5.62. UV–visible (CH$_2$Cl$_2$): λ_{max} (log ϵ), 434.5 (4.94), 568.2 (4.03), 613.1 (3.74) nm. IR (Nujol): 890 cm^{-1} (ν_{P-O}). MS (m/z): [M + H]$^+$, 918; [918 – OC$_6$H$_4$OH]$^+$, 809; [M – 2OC$_6$H$_4$OH]$^+$, 699 (base peak).

[P(TTP)(NH-p-C$_6$H$_4$CH$_3$)$_2$]Cl (18). [P(TTP)Cl$_2$]Cl (1) (0.100 g) and p-toluidine (1.330 g) were dissolved in pyridine and the solution was stirred for 24 h at room temperature. During this time the solution changed in color from dark purple to purple-brown. The solvent was removed, and the residue was chromatographed on silica gel (100 g). Elution with methanol–dichloromethane (1:9) removed a purple band, which, upon removal of the solvent, was shown by ^{1}H NMR spectroscopy to contain the desired product and a small amount of [P(TPP)Cl$_2$]Cl (1). The crude product was dissolved in benzene and left to stand. The [P(TTP)Cl$_2$]Cl impurity crystallized as purple crystals, which were filtered off. The desired product contained in the filtrate was recrystallized from benzene–octane to give a purple-brown powder (0.087 g, 76%). Anal. Calcd for C$_{62}$H$_{52}$ClN$_6$P·3H$_2$O: C, 74.35; H, 5.84; N, 8.39. Found: C, 74.41; H, 5.92; N, 7.73. UV–visible (CH$_2$Cl$_2$): λ_{max} (log ϵ), 432.5 (5.13), 315.8 (4.15), 568.2 (3.88), 616.3 (3.68) nm. MS (m/z): [M + H]$^+$, 912; [912 – NC$_6$H$_4$CH$_3$]$^+$, 807; [M – 2NHC$_6$H$_4$CH$_3$]$^+$, 699 (base peak).

Results and Discussion

Insertion Reactions. Pyridine is the most useful solvent for the insertion of the group 15 elements into the porphyrin macrocycle.[4] The use of POCl$_3$ for insertion of phosphorus into TPP has been described,[12] and we found this method to be satisfactory when TTP was used as the porphyrin ligand. The free-base porphyrin was heated at reflux temperature in pyridine for 24 h in the presence of excess POCl$_3$, resulting in a good yield (83%) of [P(TTP)Cl$_2$]Cl (1). Attempts to use PCl$_3$ as the phosphorus source resulted in a much lower yield of the same product, but contaminated with impurities which could not be separated by chromatography.

Early reports described heating SbCl$_3$ in pyridine for 30 min for the insertion of antimony into Etio, MPDME[2] and OEP,[3] although the products were incorrectly characterized. We found that no insertion of antimony into H$_2$TTP could be detected even after extended heating with a large excess of SbCl$_3$ in pyridine or 4-picoline. In contrast, when SbCl$_5$ was used as the antimony source, the insertion proceded smoothly in refluxing pyridine within 30 min, yielding [Sb(TTP)Cl$_2$]$^+$ as the [SbCl$_6$]$^-$ salt (2a). Conversion to the chloride salt (2b) could be effected by passing a methanol–dichloromethane solution of 2a through an anion-exchange resin in the chloride form. Again, both salts were obtained in excellent yields.

Antimony porphyrin complexes of OEP prepared by the reaction of AsCl$_3$ with H$_2$OEP in refluxing pyridine for 30 min have been described in the literature. In one report the product is incorrectly formulated[3] while in another experimental details are not given.[4] Our attempts to insert arsenic into H$_2$TTP using AsCl$_3$ under exactly the same conditions were unfruitful, with only

free-base porphyrin being recovered even after extended reflux times. Use of AsI$_3$ as the metal carrier or DMF as the solvent gave the same result. The higher boiling solvent quinoline led to decomposition of the porphyrin. Unlike the stable compounds PCl$_5$ and SbCl$_5$, the arsenic congener AsCl$_5$ decomposes to AsCl$_3$ and Cl$_2$ above –50 °C.[17] Attempts to use another As(V) reagent, As$_2$O$_5$, or As(III) reagents in the presence of an oxidizing agent (AsCl$_3$ with pyridine N-oxide; AsI$_3$ with I$_2$) were also unsuccessful, as was a transmetalation reaction in which the labile bismuth porphyrin [Bi(TTP)]NO$_3$ (3) was treated with AsI$_3$ in pyridine. This latter approach has been used by others, where insertion of an element has been achieved by displacement of a large, labile metal already coordinated to the porphyrin ring.[6] Although some UV–visible data for an As^{V}TPP species are given in two review articles, neither a method of preparation nor experimental details accompanied these reports.[4,6]

The reagents PCl$_3$, AsCl$_3$, and SbCl$_3$ were not effective for insertion, in contrast to the +V oxidation state reagents POCl$_3$ and SbCl$_5$, which inserted cleanly and in good yield. This contrasts with the reported insertions of the +III reagents (P, As, and Sb) into octaalkylporphyrin ligands,[2–4,9,14] indicating that element carriers in the lower oxidation state are more effective for this series of porphyrins, while those in the higher oxidation state are required for the tetraaryl series. The insertion of PCl$_3$ and PBr$_3$ into OEP and MPDME[9,14] was proposed to procede via initial insertion to form a phosphorus(III) porphyrin species, identified by a *hyper* UV–visible spectrum, followed by air[9] or Br$_2$[14] oxidation and subsequent hydrolysis to the P(V) product [P(Por)(OH)$_2$]$^+$. Where a P(V) reagent was used as the phosphorus source, reduction to P(III) prior to insertion was proposed.[4] Our attempts to use a P(III) reagent in the insertion reaction were followed by UV/visible spectroscopy, and a *hyper* type spectrum was not observed at any stage. This is an indication that the octaalkyl- and tetraarylporphyrins may require element carriers in different oxidation states for effective insertion. In fact, complexes containing the more electron-rich OEP ligand usually show electrochemical reduction potentials some 200 mV more negative than those for the corresponding TPP complexes.[18] The more easily reduced tetraarylporphyrin series may be less able to support a coordinated group 15 element in the lower +III oxidation state.

Bismuth is most stable in the +III oxidation state, a reflection of the inert pair effect observed for the heaviest elements of the main group. We found that a modification of the procedure described for the preparation of [Bi(OEP)]NO$_3$ (although incorrectly characterized in the report)[3] is effective for the synthesis of [Bi(TTP)]NO$_3$ (3). After Bi(NO$_3$)$_3$ was refluxed with H$_2$TTP in pyridine for 30 min, crystals of 3 were isolated in 72% yield. UV–visible data have been previously reported for 3 although no experimental data were given.[4]

Complexes 1–3 are air-stable in both the solid state and solution. The phosphorus complex 1 is more resistant to demetalation in weakly acidic or basic solution than the antimony congener 2. Complex 3 is rather more sensitive toward demetalation than 1 and 2, this lability reflecting the large size of the Bi(III) cation (ionic radius 0.96 Å) relative to the porphyrin ring cavity (centroid–N distance 1.98–1.05 Å).[19] Complexes 1–3 and all other species reported below were characterized by elemental analysis, UV–visible and NMR spectroscopy, and mass spectrometry.
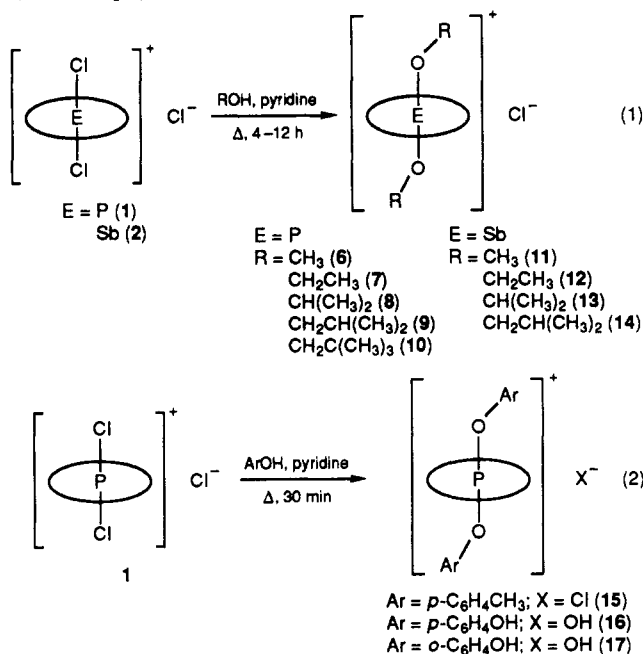
Hydroxo, Alkoxo, and Aryloxo Derivatives. Our interest in this chemistry was to examine in greater depth the reactivity of the group 15 porphyrin systems by preparing a range of derivatives of [P(TTP)Cl$_2$]$^+$ (1') and [Sb(TTP)Cl$_2$]$^+$ (2'). We achieved hydroxo-substituted derivatives of 1 and 2a by heating each complex in aqueous pyridine for 12 h, producing [P(TTP)(OH)$_2$]OH (4) and [Sb(TTP)(OH)$_2$]OH (5), respectively. The treatment of 1 or 2 with excess alkyl alcohol in refluxing pyridine for 4–12 h results in a series of alkoxo-substituted complexes

(17) Seppelt, K. *Angew. Chem., Int. Ed. Engl.* **1976**, *15*, 691.
(18) Davis, D. G. In *The Porphyrins*; Dolphin, D., Ed.; Academic Press: New York, 1978; Vol. 5, Chapter 4.
(19) Scheidt, W. R. In *The Porphyrins*; Dolphin, D., Ed.; Academic Press: New York, 1978; Vol. 3, Chapter 10.

[E(TTP)(OR)$_2$]Cl (**6–14**, eq 1). The reactions of the phosphorus complex **1** with aryl alcohols (HOAr) for 30 minutes in refluxing pyridine produce the aryloxo complexes [P(TTP)(OAr)$_2$]X (**15–17**, eq 2).

E = P (**1**)
Sb (**2**)

E = P
R = CH$_3$ (**6**)
CH$_2$CH$_3$ (**7**)
CH(CH$_3$)$_2$ (**8**)
CH$_2$CH(CH$_3$)$_2$ (**9**)
CH$_2$C(CH$_3$)$_3$ (**10**)

E = Sb
R = CH$_3$ (**11**)
CH$_2$CH$_3$ (**12**)
CH(CH$_3$)$_2$ (**13**)
CH$_2$CH(CH$_3$)$_2$ (**14**)

Ar = p-C$_6$H$_4$CH$_3$; X = Cl (**15**)
Ar = p-C$_6$H$_4$OH; X = OH (**16**)
Ar = o-C$_6$H$_4$OH; X = OH (**17**)

In contrast, reaction of the antimony analogue **2** with HO-p-C$_6$H$_4$CH$_3$ in pyridine resulted in demetalation after just 30 min at room temperature. Reaction of **2** with the salt KO-p-C$_6$H$_4$CH$_3$ produced only the Sb hydroxo complex (**5**). Complexes **4**, **6**, **7**, or **15** can also be prepared by addition of excess water or the corresponding alcohol to the solution obtained from the insertion reaction without isolation of **1**. However this results in lower yields and is accompanied by significant demetalation, probably as a result of HCl generated by reaction of water or alcohol with excess POCl$_3$.

The antimony complexes tend to be more chemically reactive than their phosphorus counterparts, and the reactions forming **11–14** are correspondingly more sensitive to reaction conditions and workup procedures. Some demetalation often occurred before conversion of [Sb(TTP)Cl$_2$]$^+$ (**2′**) to the alkoxo product was complete, and chromatographic separation of unreacted **2** from product proved difficult. The antimony species **11–14** are more sensitive to demetalation in both acidic and basic media than are their phosphorus analogues. This is also illustrated by the failure to produce an antimony aryloxo complex by the reaction of **2** with a more reactive aryl alcohol. Use of the acidic aryl alcohol leads to demetalation, while the basic aryloxo salt gave only the hydroxo-substituted derivative (**5**).

All the group 15 porphyrin complexes in the +V oxidation state reported thus far are symmetric with respect to axial ligation. An attempt was made to synthesize an unsymmetrical complex [P-(TTP)Cl(OR)]$^+$ by reaction of **1** with just 1 equiv of CH$_3$OH or CH$_3$CH$_2$OH in pyridine. Even under mild conditions (stirring at room temperature) the result was a 1:1 mixture of unreacted **1** and either **6** or **7**, respectively, indicating either that the second substitution reaction is significantly faster than the first or that a strong driving force toward symmetrization leads to intermolecular ligand exchange in any unsymmetrical complex formed. In an attempt to observe ligand exchange, the methoxo complex **6** was treated with excess ethanol in refluxing pyridine, but none of the ethoxo complex **7** was formed. The complementary reaction, that of **7** with excess methanol, was similarly unsuccessful in producing **6**.

Complex **16**, [P(TTP)(O-p-C$_6$H$_4$OH)$_2$]OH, was prepared from the reaction of **1** with excess dihydroquinone. The reaction was repeated but with a limited amount (1.0 or 0.5 equiv) of dihydroquinone in the hope of producing an oligomeric complex linked through the para-substituted dihydroxyphenyl group.

However, neither this approach nor the reaction of preformed **16** with the dichloro complex **1** in various molar ratios was successful in producing dimeric or oligomeric species. Electrostatic repulsion between the cationic monomeric complexes may present a significant barrier to these reactions.

An Arylamido Phosphorus Porphyrin Complex. The success in substituting the chloro ligands in **1** and **2** by oxygen donor ligands prompted attempts to extend this chemistry to other derivatives. When **1** was treated with excess p-toluidine in pyridine at room temperature for 24 h (eq 3), the bis(p-tolylamido)-phosphorus porphyrin complex (**18**) was isolated in 76% yield. Complete conversion was never achieved in this reaction, and an increase in the amount of p-toluidine, the reaction time or the temperature did not increase the conversion but rather promoted demetalation and decomposition.

Ar = p-C$_6$H$_4$CH$_3$ (**18**)
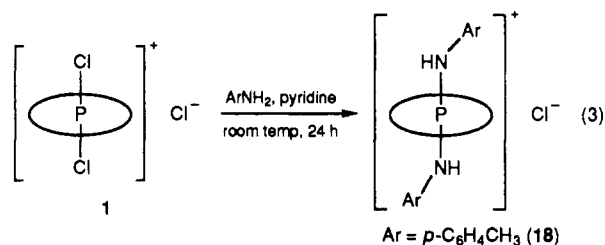
Strangely, this reaction could not be extended to other amines. Complex **1** was very reactive towards aniline, diphenylamine, piperidine, pyrrole, and a variety of other aromatic or aliphatic amines under similar conditions, but tractable products could not be isolated, and both demetalation and decomposition of the porphyrin macrocycle were the most usual outcomes. Ammonium chloride was unreactive toward **1** in pyridine. Finally, NH(Si-(CH$_3$)$_3$)$_2$ was used as a potential source of an NH fragment which would result from elimination of the stable molecules ClSi(CH$_3$)$_3$ or CH$_3$OSi(CH$_3$)$_3$ in a reaction of the reagent with **1** or **6**, respectively. Although these systems were reactive in pyridine at room temperature as indicated by the appearance of peaks in the ^{1}H NMR spectra shifted upfield of TMS by the porphyrin ring current effect, all attempts to isolate or purify the products were unsuccessful.

Reactions of this type between phosphorus(V) halides and ammonia or primary amines are well established in the chemistry of phosphazenes.[20] For example, R$_2$PCl$_3$ reacts with ArNH$_2$ to give ArN=P(R)$_2$NHAr, suggesting that compound **18** potentially could be deprotonated to form a neutral phosphinimine, ArN=P(TTP)NHAr (Ar = p-C$_6$H$_4$CH$_3$). Experimentally, this was approached by treating **18** with DBU or triethylamine in benzene, at both room temperature and elevated temperatures. However, workup resulted in nothing but starting material (**18**), and the ^{1}H NMR and UV–visible spectra were unchanged in both basic and acidic solution (in contrast to the hydroxo complex **4** which shows a marked shift in the UV–visible spectrum recorded in basic solution). A new fast-moving spot was observed by analytical thin layer chromatography of **18** under basic conditions. This is consistent with the presence of a neutral, less polar species such as the target phosphinimine complex. Unfortunately, on a preparative scale such a complex could not be isolated, and only the starting material (**18**) could be recovered on workup.

A reaction analogous to the formation of **18** was tried with p-toluidine and the antimony complex **2**. Stirring at room temperature in pyridine for 24 h produced no reaction, but even gentle heating induced demetalation. Similarly, treatment of **1** with either phenylphosphine or diphenylphosphine in pyridine at room temperature, with the aim of preparing the phosphido-substituted analogue of **18**, resulted only in demetalation and decomposition of the porphyrin. The reactivity of **1** toward sulfur compounds is illustrated by its reaction with an ethanolic solution of NaSH,[21] which in pyridine at room temperature produced the ethoxo-substituted complex **7** almost immediately. This contrasts with

(20) Neilson, R. H.; Wisian-Neilson, P. *Chem. Rev.* **1988**, *88*, 541.
(21) Klayman, D. L.; Griffen, T. S. *J. Am. Chem. Soc.* **1975**, *95*, 197.

Table III. ^{1}H (400 MHz) and ^{31}P (162 MHz) NMR Data for Compounds 1–18[a]

no.	formula	H_β ($^4J_{PH}$)	H_o, H_m ($^3J_{HH}$)	CH_3	axial ligands				^{31}P NMR Data
			Phosphorus Complexes						
1	[P(TTP)Cl$_2$]Cl	9.12 d (4.5)	7.86, 7.58 (7.9)	2.63 s					−179.33
4	[[P(TTP)(OH)$_2$]OH	9.11 d (br)	7.86, 7.58 (7.8)	2.63 s					−195.94
6	[P(TTP)(OCH$_3$)$_2$]Cl	9.06 d (2.7)	7.80, 7.56 (7.8)	2.63 s	OCH$_3$	−1.88	d	$^3J_{PH}$ = 25.5	−179.93
7	[P(TTP)(OCH$_2$CH$_3$)$_2$]Cl	9.06 d (2.7)	7.82, 7.57 (7.8)	2.64 s	OCH$_2$	−2.35	dq	$^3J_{PH}$ = 14.0 $^3J_{HH}$ = 7.0	−181.86
					CH$_3$	−1.76	td	$^3J_{HH}$ = 7.0 $^4J_{PH}$ = 1.7	
8	[P(TTP)(OCH(CH$_3$)$_2$)$_2$]Cl	9.13 d (2.7)	7.93, 7.61 (7.6)	2.67 s	OCH	−2.78	dsept	$^3J_{PH}$ = 2.63 $^3J_{HH}$ = 6.0	−178.31
					CH$_3$	−2.21	d	$^3J_{HH}$ = 6.0	
9	[P(TTP)(OCH$_2$CH(CH$_3$)$_2$)$_2$]Cl	9.06	7.84, 7.59 (7.8)	2.65 s	OCH$_2$	−2.75	dd	$^3J_{PH}$ = 9.5 $^3J_{HH}$ = 6.4	−181.69
					CH	−1.40	nonet	$^3J_{HH}$ = 6.4	
					CH$_3$	−1.24	d	$^3J_{HH}$ = 6.4	
10	[P(TTP)(OCH$_2$C(CH$_3$)$_3$)$_2$]Cl	9.10	7.93, 7.60 (7.4)	2.65 s	OCH$_2$	−2.99	d	$^3J_{PH}$ = 8.0	−180.30
					CH$_3$	−1.41	s		
15	[P(TTP)(O-p-C$_6$H$_4$CH$_3$)$_2$]Cl	9.01 d (3.2)	7.66, 7.52 (7.9)	2.62 s	H$_o$	2.08	dd	$^3J_{HH}$ = 7.8 $^4J_{PH}$ = 2.3	−230.33
					H$_m$	5.69	d	$^3J_{HH}$ = 7.8	
					CH$_3$	1.64	d	$^7J_{PH}$ = 2.1	
16	[P(TTP)(O-p-C$_6$H$_4$OH)$_2$]OH	8.86 d (2.9)	7.63, 7.45 (7.8)	2.51 s	H$_o$	1.85	dd	$^3J_{HH}$ = 8.5 $^4J_{PH}$ = 2.2	−192.03
					H$_m$	5.48	d	$^3J_{HH}$ = 8.5	
17	[P(TTP)(O-o-C$_6$H$_4$OH)$_2$]OH	8.91 d (3.5)	7.70, 7.41 (7.6)	2.56 s	H$_o$	1.04	d	$^3J_{HH}$ = 8.0	−195.19
					H$_m$	5.26		$^3J_{HH}$ = 8.0	
					H$_p$	5.88		$^3J_{HH}$ = 8.0	
					H$_{m'}$	5.76		$^3J_{HH}$ = 8.0	
18	[P(TTP)(NH-p-C$_6$H$_4$CH$_3$)$_2$]Cl	8.87 d (2.0)	7.68, 7.46 (7.6)	2.58 s	H$_o$	2.14	dd	$^3J_{HH}$ = 7.6 $^4J_{PH}$ = 2.0	−209.69
					H$_m$	5.66	d	$^3J_{HH}$ = 7.6	
					CH$_3$	1.62	d	$^7J_{PH}$ = 1.3	
			Antimony and Bismuth Complexes						
2a	[Sb(TTP)Cl$_2$]SbCl$_6$	9.64 s	8.24, 7.76 (7.9)	2.78 s					
2b	[Sb(TTP)Cl$_2$]Cl	9.63 s	8.23, 7.77 (7.9)	2.79 s					
5	[Sb(TTP)(OH)$_2$]OH	9.33 s	8.15, 7.59 (7.8)	2.73 s					
11	[Sb(TTP)(OCH$_3$)$_2$]Cl	9.57 s	8.20, 7.74 (7.9)	2.78 s	OCH$_3$	−2.20	s		
12	[Sb(TTP)(OCH$_2$CH$_3$)$_2$]Cl	9.64 s	8.20, 7.74 (7.9)	2.78 s	OCH$_2$	−2.29	q	$^3J_{HH}$ = 6.6	
					CH$_3$	−2.21	t	$^3J_{HH}$ = 6.6	
13	[Sb(TTP)(OCH(CH$_3$)$_2$)$_2$]Cl	9.53 s	8.16, 7.73 (7.7)	2.78 s	OCH	−3.38	sept	$^3J_{HH}$ = 6.1	
					CH$_3$	−2.52	d	$^3J_{HH}$ = 6.1	
14	[Sb(TTP)(OCH$_2$CH(CH$_3$)$_2$)$_2$]Cl	9.54 s	8.15, 7.74 (7.8)	2.79 s	OCH$_2$	−2.90	d	$^3J_{HH}$ = 6.7	
					CH	−1.99	m		
					CH$_3$	−1.68	d	$^3J_{HH}$ = 6.6	
3	[Bi(TTP)]NO$_3$	9.19 s	8.11, 7.58 (br)	2.73 s					

[a] All spectra were recorded in CDCl$_3$ solution. Chemical shifts are reported in ppm downfield from internal tetramethylsilane. Coupling constants are reported in Hz. Key: s = singlet, d = doublet, t = triplet, q = quartet, sept = septet, and m = multiplet.

the 12 h in refluxing pyridine–ethanol required to produce **7** directly and indicates that NaSH may attack **1** to produce a very reactive intermediate which is then further substituted by ethanol. Either no reaction or demetalation resulted from reactions of **1** with KS-p-C$_6$H$_4$CH$_3$ or HS-p-C$_6$H$_4$CH$_3$, respectively.

Satisfactory elemental analysis data were obtained for all complexes 1–18 except for **12** and **14**, which proved difficult to purify even after repeated chromatography. These compounds were characterized on the basis of spectroscopic data. The antimony complex **13** was further characterized by an X-ray crystal structure analysis, discussed below. An investigation of the electrochemistry and spectroelectrochemistry of [E(TTP)Cl$_2$]Cl (E = P (**1**), Sb (**2b**)) and [E(TTP)(OCH$_3$)$_2$]Cl (E = P (**6**), Sb (**11**)) is the subject of a separate report.[22]

UV–Visible Spectra. The P and Sb porphyrin complexes **1**, **2**, and **4–18** all exhibit normal UV–visible spectra, with a Soret band in the range 423–443 nm and two less intense bands in the visible region. The Soret bands of the phosphorus aryloxo and p-tolylamido complexes **15–18** are broader and less intense than

those of the chloro-, hydroxo-, and alkoxo-substituted congeners. The bismuth(III) complex **3** shows a *hyper* spectrum, with the Soret band at 469 nm. [P(TTP)(OH)$_2$]OH (**4**) exhibits acid–base behavior in solution. A pure sample of **4** dissolved in CH$_2$Cl$_2$ solution shows the presence of two species, the first with a Soret band at 431 nm and weaker visible bands at 557 and 600 nm and the second with bands at 453 (Soret) and 651 (visible) nm. In neat pyridine only one species is present, and the spectrum simplifies to show only the bands at 431 (Soret), 557, and 600 nm. The same result is observed if excess triethylamine or DBU is added to the CH$_2$Cl$_2$ solution, and subsequent dropwise addition of dilute acetic acid re-forms the original mixture. Two successive deprotonations of the water-soluble complex [P(MesoDME)- (OH)$_2$]$^+$ have been observed.[14] Compound **5** (the antimony analogue of **4**) and compounds **16–18**, which also have potentially ionizable protons, show identical UV–visible spectra in acidic and basic solution.

NMR Spectra. ^{1}H and ^{31}P NMR data for complexes 1–18 are collected in Table III. ^{1}H NMR spectra of the phosphorus complexes **1**, **4**, **6–10**, and **15–18** each show a β-pyrrolic peak in the range 8.86–9.12 ppm which appears as doublet due to coupling with the central phosphorus atom ($^4J_{HP}$ = 2.0 – 4.5 Hz). In the antimony species **2**, **5**, and **11–14** the β-pyrrolic resonance is a

(22) Liu, Y. H.; Bénassy, M.-F.; Barbour, T.; Belcher, W. J.; Brothers, P. J.; Kadish, K. M. Manuscript in preparation.

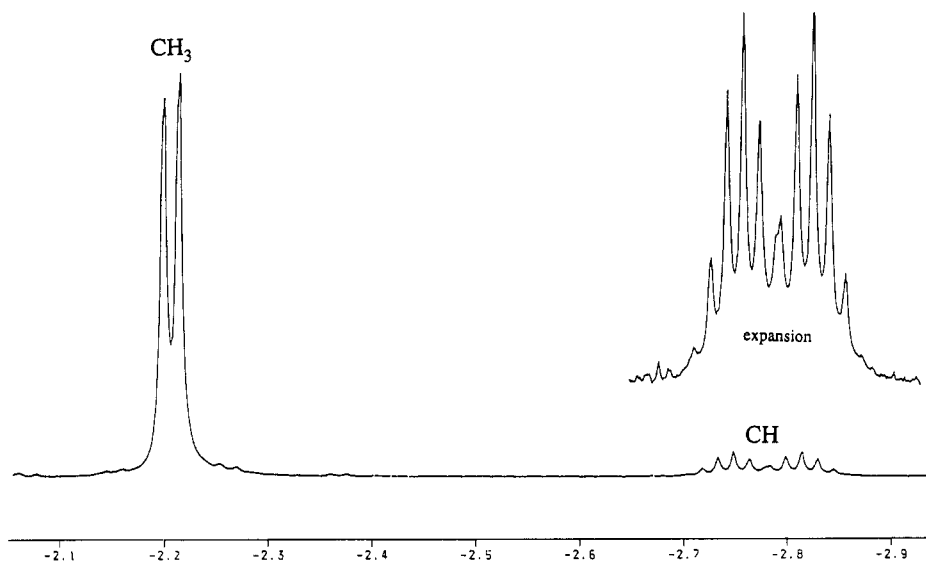**Figure 1.** High-field region of the ^1H NMR spectrum (400 MHz, $CDCl_3$) of $[P(TTP)(OCH(CH_3)_2)_2]Cl$ (**8**).

singlet in the range 9.33–9.64 ppm. In all the P and Sb complexes the ortho and meta protons of the *p*-tolyl substituents on the porphyrin periphery appear as a pair of doublets, indicative either of a complex with two equivalent axial ligands or of rapid rotation of the *p*-tolyl groups on the NMR time scale. ^1H NMR resonances for the axial ligands, together with elemental analysis data and the crystal structure of the antimony complex [Sb(TTP)(O-CH(CH₃)₂)₂]Cl (**13**) (vide infra), are all consistent with the P and Sb complexes having two equivalent axial ligands. The room-temperature ^1H NMR spectrum of the bismuth complex **3a**, on the other hand, shows broad, poorly resolved peaks for the *p*-tolyl ortho and meta protons. Kinetic data from a variable-temperature ^1H NMR study of **3** will be analyzed in detail in a later section.

Resonances arising from the axial ligands in the P and Sb complexes are typically shifted upfield of their normal ranges due to the porphyrin diamagnetic ring current effect. For example, the P (Sb) isopropoxo complexes **8** (**13**) show CH resonances at −2.78 (−3.38) ppm (septet), and CH₃ resonances at −2.21 (−2.52) ppm (doublet), respectively. The upfield region of the ^1H NMR spectrum of **8** is shown in Figure 1. The P complexes **6–9** show additional three-bond coupling between the central P atom and the protons on the α-carbon of the alkoxo group ($^3J_{HP}$ = 9.5–26.3 Hz). In the case of the ethoxo complex **7** four-bond coupling (1.7 Hz) to the methyl protons is also resolved. Long-range coupling from the central P atom to protons in the axial ligands is especially marked in complexes **15, 16,** and **18,** in which the axial ligands contain aryl groups. Coupling to the ortho protons is observed in these three compounds ($^4J_{HP}$ = 2.0–2.3 Hz), and in **15** and **18** remarkable seven-bond coupling between P and the methyl protons on the axial *p*-tolyl groups is observed ($^7J_{HP}$ = 1.3–2.1 Hz). Complexes **15** and **16,** derived from 1,4-hydroxymethylbenzene and 1,4-dihydroxybenzene, respectively, show one resonance for each pair of ortho and meta protons on the axial ligands. The isomer of **16** derived from 1,2-dihydroxybenzene (**17**) shows four distinct resonances for the four chemically different protons in the ligand, each integrating for two protons. The OH protons in neither the ligands nor the counterions of complexes **4, 5, 16,** and **17** are observed, due to rapid exchange with trace amounts of water in the solvent. However the NH protons in the *p*-tolylamido complex **18** appear as a doublet at −2.03 ppm ($^2J_{HP}$ = 14.8 Hz) which disappears on addition of D₂O.

A resonance for the coordinated P atom was observed in the $^{31}P\{^1H\}$ NMR spectrum of each of complexes **1, 4, 6–10,** and **15–18** as a singlet in the range −178 to −230 ppm (relative to external 85% H₃PO₄). This marked upfield shift relative to the P(V) reference is again attributed to the porphyrin ring current. A proton-coupled ^{31}P NMR spectrum of [P(TTP)(OCH₃)₂]Cl (**6**) shows both the three-bond coupling between P and the six methoxo

Table IV. Selected Bond Lengths (Å) and Angles (deg) for [Sb(TTP)(OCH(CH₃)₂)₂]Cl (**13**)

Bond Lengths			
Sb–O1	1.929 (7)	O1–C48	1.436 (11)
Sb–O2	1.940 (7)	C48–C49	1.48 (2)
Sb–N1	2.091 (9)	C48–C50	1.44 (3)
Sb–N2	2.075 (9)	O2–C45	1.416 (15)
Sb–N3	2.065 (9)	C45–C46	1.531 (16)
Sb–N4	2.073 (9)	C45–C47	1.50 (2)

Bond Angles			
O1–Sb–O2	172.3 (3)	N1–Sb–N4	178.6 (3)
Sb–O1–C48	125.3 (7)	N1–Sb–N3	89.8 (4)
O1–C48–C49	108.9 (11)	N2–Sb–N4	90.0 (3)
O1–C48–C50	108.9 (12)	N1–Sb–O1	87.5 (3)
C49–C48–C50	113.3 (14)	N2–Sb–O1	93.6 (3)
Sb–O2–C45	126.8 (6)	N3–Sb–O1	86.4 (3)
O2–C45–C46	109.9 (10)	N4–Sb–O1	91.2 (3)
O2–C45–C47	109.5 (11)	N1–Sb–O2	94.9 (3)
C46–C45–C47	112.8 (10)	N2–Sb–O2	93.9 (3)
N1–Sb–N2	89.6 (4)	N3–Sb–O2	86.1 (3)
N2–Sb–N3	179.4 (3)	N4–Sb–O2	90.4 (3)
N3–Sb–N4	90.6 (4)		

protons (25.5 Hz) and the four-bond coupling to the eight β-pyrrolic protons, resulting in a 63-line multiplet for the phosphorus resonance (Figure 2).

Infrared and Mass Spectra. The P–Cl stretching frequency observed at 425 cm⁻¹ in the IR spectrum (Nujol mull) of [P-(TTP)Cl₂]Cl (**1**) was not present in the spectra of the derivatives **4, 6–10,** and **15–18.** In these complexes ν_{PO} was observed in the range 885–903 cm⁻¹ for **4** and **15–17** and near 1040 cm⁻¹ (partially obscured by porphyrin ligand bands) in **6** and **7.** For the Sb complex [Sb(TTP)Cl₂]SbCl₆ (**2a**), ν_{SbCl} is assigned at 350 cm⁻¹ for the metalloporphyrin cation and at 325, 330, and 335 cm⁻¹ for the SbCl₆⁻ anion, the latter distorted from perfect octahedral symmetry.[23] Only the 350-cm⁻¹ band is apparent in the far-IR spectrum of the chloride salt **2b.** No activity is observed in the far IR region of the spectra of the alkoxo-substituted complexes **11–14.** Other bands, namely $\delta_{Sb–OH}$ (1070 cm⁻¹) and $\nu_{Sb–O}$ (585 cm⁻¹) were assigned for **5** and **11,** respectively, by comparison with data for the other antimony compounds.[23] Bands due to water, ν_{OH} near 3400 cm⁻¹ and δ_{OH} at 1610 cm⁻¹ were observed in the IR spectra of all complexes where the elemental analysis figures indicated the presence of water of crystallization in the solid samples.

Although the volatility of these cationic complexes is very low, fast atom bombardment (FAB) mass spectrometry was effective

(23) Nakamoto, K. *Infrared and Raman Spectra of Inorganic and Coordination Compounds,* 3rd ed.; Wiley: New York, 1978.
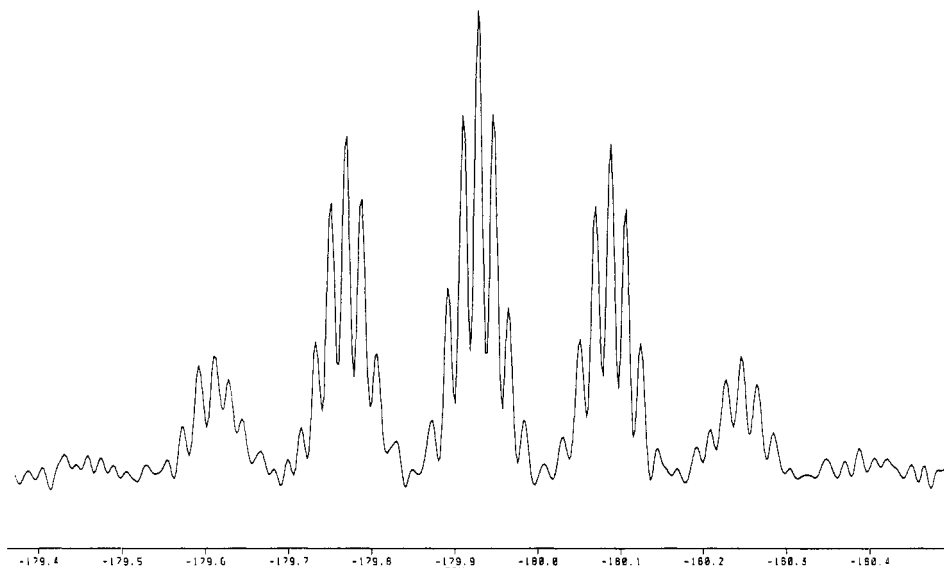
Figure 2. Proton-coupled ^{31}P NMR spectrum (162 MHz, $CDCl_3$) of [P(TTP)(OCH$_3$)$_2$]Cl (6).
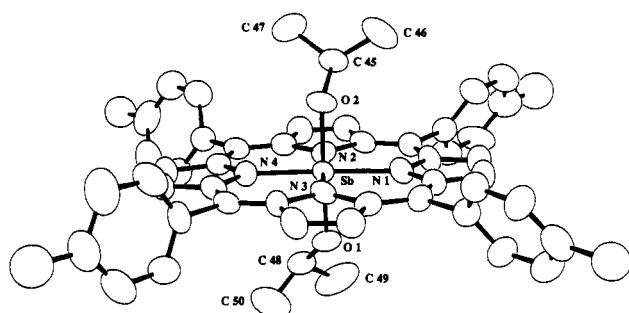
Figure 3. Drawing of the cation of [Sb(TTP)(OCH(CH$_3$)$_2$)$_2$]Cl (13) (hydrogen atoms omitted). Atoms are represented as 50% probability ellipsoids.

in obtaining spectra of the complexes. Molecular ion peaks corresponding to the cationic porphyrin species were observed for most complexes. Ions corresponding to loss of R and OR from [E(TTP)(OR)$_2$]$^+$ and species assigned as [E(TTP)=O]$^+$ (m/z

= 715, E = P; m/z = 805, E = ^{121}Sb) and [E(TTP)]$^+$ (m/z = 699, E = P; m/z = 791, E = ^{123}Sb; m/z = 789, E = ^{121}Sb) were commonly identified in the fragmentation patterns. Loss of propene (C$_3$H$_6$) from both the phosphorus and antimony iso-propoxo cations 8 and 13, respectively, was also observed.

Structure of [Sb(TTP)(OCH(CH$_3$)$_2$)$_2$]Cl (13). Crystals of 13 were prepared by slow recrystallization of the complex from dichloromethane–toluene–octane. A drawing of the [Sb-(TTP)(OCH(CH$_3$)$_2$)$_2$]$^+$ cation is shown in Figure 3 and selected bond lengths and angles are given in Table IV. The antimony atom exhibits approximate octahedral geometry, lying 0.030 Å out of the mean porphyrin plane (0.019 Å out of the mean N$_4$ plane) toward O2. The position of the relatively small chloride counterion is disordered and occupies more than one position within the larger cavities between the metalloporphyrin cations.

The Sb–O bond lengths are almost equivalent, averaging to 1.935 Å, and compare well with the Sb–O bond length of 1.938 (4) Å observed in [Sb(TTP)(OH)$_2$]ClO$_4$·CH$_3$CH$_2$OH, the only other structurally characterized antimony porphyrin complex.[7] The O–Sb–O bond angle of 172.3 (3)° is more distorted from
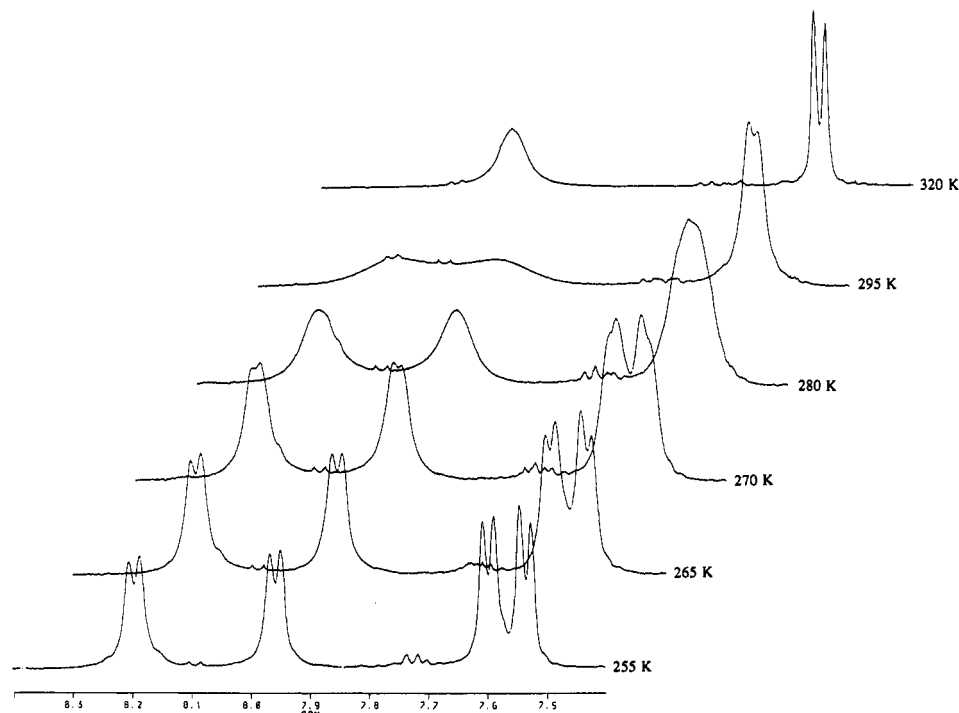

Figure 4. ^{1}H NMR spectra (400 MHz, $CDCl_3$) showing *p*-tolyl H$_o$ and H$_m$ protons of [Bi(TTP)]NO$_3$ (3) in the temperature range 255–320 K.

linearity than the corresponding angle of 178° found in [Sb-(TTP)(OH)$_2$]$^+$, probably as a consequence of the bulkier isopropoxo ligands present in **13**. The average Sb–N bond lengths for **13** and [Sb(TTP)(OH)$_2$]$^+$ are 2.076 and 2.074 Å, respectively. Both the Sb–O and average Sb–N bond lengths in **13** are slightly shorter than the Sn–O (2.00 (3), 2.035 (5) Å) and the average Sn–N (2.09 (5) Å) bond distances observed in the isoelectronic Sn(IV) complex Sn(TTP)(OH)$_2$·2CHCl$_3$·2CCl$_4$.[24] The Sb–O1–C46 and Sb–O2–C45 bond angles of 125.3 (7) and 126.8 (6)°, respectively, are larger than the tetrahedral angle of 109.5°. Again, this is most likely a consequence of the steric bulk of the axial ligands. Similar angles of 126.4 (2) and 124.0 (3)° are observed for the Ge–O–C angle in Ge(TPP)(OCH$_2$CH$_3$)$_2$[25] and Ge(Por)(OCH$_3$)$_2$.[26] The isopropyl groups in **13** are oriented with the two methyl substituents directed away from the porphyrin macrocycle.

Variable-Temperature ^{1}H NMR Study of [Bi(TTP)]NO$_3$ (3). Compound **3** exhibits a temperature-dependent ^{1}H NMR spectrum in both chloroform and acetone solution. In particular the aromatic protons of the tolyl groups on the periphery of the porphyrin ring appear very broadened in the room-temperature spectrum (295 K). In contrast, these protons appear as two sharp doublets in the ^{1}H NMR spectra of the phosphorus and antimony complexes. ^{1}H NMR spectra of **3** were observed over a range of temperatures. The aromatic tolyl resonances in these spectra are shown in Figure 4. At low temperature (255 K) four broad doublets appear, while at the highest temperature observed (320 K) these have collapsed to two peaks. The high-temperature limit at which two sharp doublets would be expected was not accessible in the solvent used. A kinetic line shape analysis of the spectra gives a value of $\Delta G^{\ddagger}$ in the range 60–64 kJ·mol^{-1} for this process. This is within the range observed for phenyl ring rotation in unsymmetrical tetraphenylporphyrin complexes of ruthenium, indium, and gallium.[27]

The phosphorus and antimony complexes, which do not exhibit this temperature dependence, bear two equivalent axial ligands and thus the symmetry plane containing the porphyrin core is retained. Even if aryl group rotation is occurring, the two sides of the aryl groups are not chemically differentiated, and thus the aromatic protons are chemically equivalent by NMR. If the dynamic behavior apparent from the ^{1}H NMR spectrum of the bismuth complex **3** does arise from tolyl ring rotation, then the symmetry plane containing the porphyrin macrocycle must have been lost. At low temperature, in the limit of slow rotation on the NMR time scale, the two pairs of protons on the tolyl ring are chemically inequivalent and give rise to four doublets in the ^{1}H NMR spectrum. At higher temperature, rotation becomes rapid on the NMR time scale, and the protons appear as only two doublets, reflecting an averaged chemical environment.

Loss of the symmetry plane containing the porphyrin could arise from two possibilities. First, the nitrate counterion may be associated with the bismuth center, chemically differentiating the two sides of the porphyrin plane. Second, the bismuth(III) ion itself is too large to fit in the porphyrin cavity and thus would not be expected to lie completely in the plane of the porphyrin. In the crystal structure of the isoelectronic complex Pb(Por) (Por = *meso*-tetra-*n*-propylporphyrin), the Pb(II) ion lies 1.174 Å above the least-squares plane through the four nitrogen atoms.[28] Similarly, the Tl(III) ion in Tl(OEP)Cl lies 0.69 Å above the plane of the four nitrogen atoms.[29] The Bi(III) ionic radius (0.96 Å) is similar to that of Tl(III) (0.95 Å), and thus an out-of-plane geometry would be expected for [Bi(TTP)]NO$_3$. The asymmetry about the porphyrin plane could then derive simply from out-of-plane coordination of the metal atom.

Summary. Complexes encompassing the non-metal element phosphorus through to the heavy-metal element bismuth have been prepared and fully characterized. The reactions of the phosphorus and antimony complexes with alcohols and an amine have extended the range of group 15 porphyrin species to include alkoxo and aryloxo complexes and a phosphorus arylamido complex, which contains this element octahedrally coordinated to six nitrogen atoms. A variable-temperature NMR study of [Bi(TTP)]NO$_3$ illustrates the lack of symmetry in the plane of the porphyrin in this complex.

(24) Harrison, P. G.; Molloy, K.; Thornton, E. W. *Inorg. Chim. Acta* **1979**, *33*, 137.

(25) Balch, A. L.; Cornman, C. R.; Olmstead, M. M. *J. Am. Chem. Soc.* **1990**, *112*, 2963.

(26) Mavridis, A.; Tulinsky, A. *Inorg. Chem.* **1976**, *15*, 2723.

(27) Eaton, S. S.; Eaton, G. R. *J. Am. Chem. Soc.* **1977**, *99*, 6594.

(28) Barkigia, K. M.; Fajer, J.; Adler, A. D.; Williams, G. J. B. *Inorg. Chem.* **1980**, *19*, 2057.

(29) Cullen, D. L.; Meyer, E. F.; Smith, K. M. *Inorg. Chem.* **1977**, *16*, 1179.